CHAOTIC OSCILLATIONS OF A SPHERICAL PENDULUM AS AN EXAMPLE OF INTERACTION WITH AN ENERGY SOURCE

T. S. Krasnopol'skaya and A. Yu. Shvets

UDC 534.1

A spherical pendulum is the simplest example of an oscillator with two degrees of freedom of equal frequency. Many of the phenomena typical of the behavior of a spherical pendulum also show up in the dynamics of systems with distributed parameters with a periodic coordinate. Examples include rings, cylindrical and spherical shells, circular plates, and media inside cylindrical and spherical cavities. Therefore knowledge of the properties of a spherical pendulum gives an understanding of oscillations in these other systems.

In the present paper we consider of the chaotic motion of deterministic parametric oscillations of a kinematically driven spherical pendulum. It is shown that chaotic oscillations result from the interaction of the pendulum with a driving mechanism of finite power. The generation of chaos caused by interaction with the driving mechanism is studied using averaged equations of motion which closely approximate the behavior of real systems [4]. In the case of an ideal (infinite power) driving mechanism the averaged equations describing parametric oscillations of a spherical pendulum have only regular solutions in the steady state [9, 10]. The change in the type of dynamical system (the pendulum) from deterministic [3] (having only regular motion) to chaotic (capable of dynamical chaos) due to interaction with an energy source shows the importance of properly taking into account the interaction process. This is particularly true for experimental studies of the properties of dynamical systems. Chaos in the system can be caused only by the finiteness of the power of the driving mechanism, and not by the properties of the system itself.

We consider the system show schematically in Fig. 1a. A crank-shaft slide bar mechanism connects the rotor of a motor with the point of support of a physical pendulum. When the crankshaft a turns by an angle ψ the slide bar together with the support (when the length of the connecting rod b >> a) suffers a displacement $v(t) = -a\cos\psi$ along the vertical axis of a fixed coordinate system. In Cartesian coordinates xyz the kinetic energy can be written in the form [1, 2, 7, 8] (in a fixed coordinate system)

$$T = \frac{1}{2} I\dot{\psi}^2 + \frac{1}{2} m\,[\dot{x}^2 + \dot{y}^2 + (\dot{z} + \dot{v})^2], \tag{1}$$

and the potential energy has the form

$$V = mg\,(l - z - v), \tag{2}$$

where x, y, z are the Cartesian coordinates of the center of mass of the pendulum; I is the moment of inertia of the rotor of the electric motor; m is the mass of the pendulum; and ℓ is the reduced length of the pendulum. The masses of the slide bar and support are neglected.

Following [7], we introduce the new variables α and β defined as $x = \ell\sin\alpha$, $y = \ell\sin\beta$. Because for a pendulum we always have the relation $x^2 + y^2 + z^2 = \ell^2$, it follows that $z = \ell\sqrt{1 - \sin^2\alpha - \sin^2\beta}$. For small α and β the Lagrangian of the system $L = T - V$ can be written in the form [2, 7, 8]:

$$L = \frac{1}{2} I\dot{\psi}^2 + \frac{1}{2} ml^2\left\{\dot{\alpha}^2 + \dot{\beta}^2 + 2\alpha\beta\dot{\alpha}\dot{\beta} - 2\,(\alpha\dot{\alpha} + \beta\dot{\beta})\,\dot{\psi}\times\right.$$

$$\left.\times\frac{a}{l}\sin\psi + \dot{\psi}^2\frac{a^3}{l^2}\sin^2\psi\right\} - gml\left(\frac{\alpha^2}{2} - \frac{\alpha^4}{24} + \frac{\beta^2}{2} - \frac{\beta^4}{24} + \frac{\alpha^2\beta^2}{4} + \frac{a}{l}\cos\psi\right); \tag{3}$$

Institute of Mechanics, Academy of Sciences of the Ukraine, Kiev. Translated from Prikladnaya Mekhanika, Vol. 28, No. 10, pp. 61-68, October, 1992. Original article submitted January 29, 1991.

1063-7095/92/2810-0669$12.50

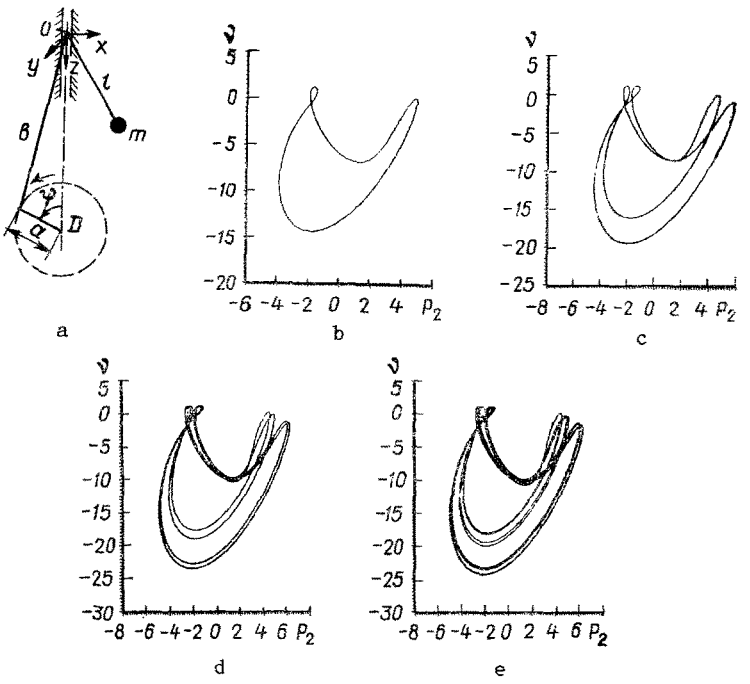

Fig. 1

Lagrange's equations for the basic variables $\psi(t)$, $\alpha(t)$, and $\beta(t)$ take the form

$$
\begin{aligned}
&I\ddot{\psi} = H_1(\dot{\psi}) - H_2(\dot{\psi}) - mla\left[\ddot{\psi}\frac{a}{l}\sin^2\psi + \dot{\psi}^2\frac{a}{l}\sin\psi\cos\psi + \frac{g}{l}\sin\psi - \right.\\
&\left. - (\dot{\alpha}^2 + \dot{\beta}^2)\sin\psi - (\alpha\ddot{\alpha} + \beta\ddot{\beta})\sin\psi\right];\\
&\ddot{\alpha} + \omega_0^2\left(\alpha - \frac{\alpha^3}{6} + \frac{\alpha\beta^2}{2}\right) + \delta_1\dot{\alpha} + \alpha(\dot{\beta}^2 + \beta\ddot{\beta}) - \\
&- \frac{a}{l}\alpha(\dot{\psi}^2\cos\psi + \ddot{\psi}\sin\psi) = 0;\\
&\ddot{\beta} + \omega_0^2\left(\beta - \frac{\beta^3}{6} + \frac{\alpha^2\beta}{2}\right) + \delta_1\dot{\beta} + \beta(\dot{\alpha}^2 + \alpha\ddot{\alpha}) - \\
&- \frac{a}{l}\beta(\dot{\psi}^2\cos\psi + \ddot{\psi}\sin\psi) = 0.
\end{aligned}
\tag{4}
$$

Here $H_1(\dot{\psi})$ is the torque of the electric motor; $H_2(\dot{\psi})$ is the internal torque of resistance to the rotation of the rotor; $\omega_0 = (g/\ell)^{1/2}$ is the natural frequency of the pendulum; δ_1 is the damping coefficient of the drag force of the medium in which the pendulum moves.

The above equations describe the complicated interaction between the rotation of the shaft of the motor (producing the driving force) and the spatial oscillations of the pendulum. The equations are essentially nonlinear and cannot be solved analytically. To simplify (4) we introduce the small parameter $\varepsilon = a/\ell$, where we assume that $a \ll \ell$. In addition, we assume fundamental parametric resonance, where the velocity $\dot{\psi}$ is close to $2\omega_0$:

$$\dot{\psi}(t) = 2\omega_0 + \varepsilon\omega_0\nu. \tag{5}$$

The resonant oscillations of the pendulum are studied using the relations

$$
\begin{aligned}
&\alpha(t) = \varepsilon^{1/2}\left[p_1(\tau)\cos\frac{\psi(t)}{2} + q_1(\tau)\sin\frac{\psi(t)}{2}\right];\\
&\beta(t) = \varepsilon^{1/2}\left[p_2(\tau)\cos\frac{\psi(t)}{2} + q_2(\tau)\sin\frac{\psi(t)}{2}\right].
\end{aligned}
\tag{6}
$$

Using (6) we transform to the new variable $p_1(\tau)$, $q_1(\tau)$, $p_2(\tau)$, $q_2(\tau)$, where τ is the slow time

$$\tau = \frac{\varepsilon}{4}\psi(t). \tag{7}$$

We use the method of averaging, which simplifies the original system of equations somewhat and in some cases makes it possible to obtain analytical solutions. Without using the method of averaging it would be difficult to identify the main trends in the interaction process.

We substitute (6) into (4) and use the relations $\dot{\alpha}(t) = \varepsilon^{1/2}\frac{\dot{\psi}}{2}\left[-p_1 \sin\frac{\psi}{2} + q_1\cos\frac{\psi}{2}\right]$ and $\dot{\beta}(t) = \varepsilon^{1/2}\frac{\dot{\psi}}{2}\left[-p_2\sin\frac{\psi}{2} + q_2\cos\frac{\psi}{2}\right]$, $\left(' = \frac{d}{dt}\right)$. After averaging with respect to fast time $\psi(t)$ from 0 to 2π, we obtain

$$\begin{aligned}
\frac{d\nu}{d\tau} &= N_2 - N_1\nu - \mu(p_1q_1 + p_2q_2);\\
\frac{dp_1}{d\tau} &= -\delta p_1 - \left[\nu + \frac{1}{8}(p_1^2 + q_1^2 + p_2^2 + q_2^2)\right]q_1 - \frac{3}{4}(p_1q_2 - q_1p_2)\,p_2 + 2q_1;\\
\frac{dq_1}{d\tau} &= -\delta q_1 + \left[\nu + \frac{1}{8}(p_1^2 + q_1^2 + p_2^2 + q_2^2)\right]p_1 - \frac{3}{4}(p_1q_2 - q_1p_2)\,q_2 + 2p_1;\\
\frac{dp_2}{d\tau} &= -\delta p_2 - \left[\nu + \frac{1}{8}(p_1^2 + q_1^2 + p_2^2 + q_2^2)\right]q_2 + \frac{3}{4}(p_1q_2 - q_1p_2)\,p_1 + 2q_2;\\
\frac{dq_2}{d\tau} &= -\delta q_2 + \left[\nu + \frac{1}{8}(p_1^2 + q_1^2 + p_2^2 + q_2^2)\right]p_2 + \frac{3}{4}(p_1q_2 - q_1q_2)\,q_1 + 2p_2.
\end{aligned} \tag{8}$$

Here we use the linear approximation to the static characteristic of the motor, where

$$\frac{H_1(\dot{\psi}) - H_2(\dot{\psi})}{I + \frac{1}{2}ma^2} = \varepsilon\frac{\omega_0}{2}[N_0 - N_1\dot{\psi}] + \varepsilon^2 \ldots. \tag{9}$$

Therefore

$$N_2 = \left[\frac{N_0}{\omega_0} - 2N_1\right]\frac{l}{a},\ \text{a}\ \mu = \frac{2ml^2}{I + \frac{1}{2}ma^2},\ \delta = \frac{\delta_1}{\omega_0}.$$

The purpose of the present paper is to analyze all possible classes of steady-state motion for the system of equations (8). In practice the different types of steady-state motion can be found for (8) only with the help of numerical methods of solution.

With the help of numerical experiments, we determined the existence regions for steady-state cahotic motion of the system and analyzed the transition from regular motion to chaotic motion.

The numerical experiments were performed on the Pyramid personal computer (type IBM PC/AT-286). The basic computational method used to construct solutions of the differential equations was the fourth-order Runge–Kutta method with the use of the Prince–Dorman correction procedure. It was verified that the accuracy of the calculations was at least $0(10^{-8})$. In constructing the phase portraits of steady-state motion particular attention was paid to removing distortions caused by the trajectories of transient processes. The Poincaré sections maps were constructed with the help of Henson's method [6]. For chaotic oscillations the number of points in the sections was at least 10^4. The algorithm of Benettin et al [5] was used to construct the characteristic Lyapunov exponents. This algorithm was modified in order to eliminate the effect of atypical trajectories on the Lyapunov exponents. All of the figures shown here were obtained on the personal computer with the help of the GRAPHER program.

We consider the transition from regular to chaotic motion for the following values of the parameters of the system and initial conditions

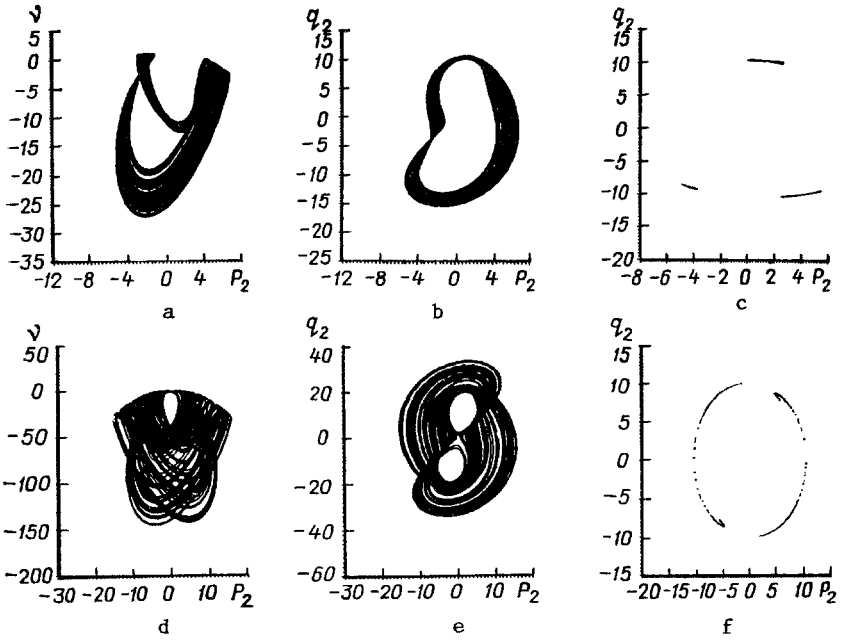

Fig. 2

$$N_2 = 0{,}5, \quad \delta = 0{,}5, \quad \mu = 1, \quad p_1 = q_1 = 0{,}1; \qquad \nu = 0, \quad p_2 = q_2 = 1. \tag{10}$$

The bifurcation parameter was taken to be the slope angle N_1 of the characteristic of the electric drive, which depends on the type of driver used. For $1.75 \geq N_1 \geq 1.43$ there exists in the system a stable one-stroke limit cycle of period 4.4. At $N_1 = 1.42$ this cycle becomes unstable and there is a stable two-stroke limit cycle of period 8.8. Further period-doubling bifurcations occur at $N_1 = 1.3$ and $N_1 = 1.28$ and the system has four and eight-stroke limit cycles with periods 17.7 and 35.3, respectively. Figure 1b-e show the projections of the phase portraits of these cycles onto the (p_2, ν) plane. A chaotic attractor occurs in the system for the critical value $N_1 = 1.27$. The projections of the phase portrait of the chaotic attractor are shown in Figs. 2a, b for $N_1 = 1.25$. Figure 2c shows the projection of the Poincaré section (by the plane $\nu = -11$) of this attractor onto the (p_2, q_2) plane. The leading Lyapunov exponent for the chaotic attractor shown in Fig. 2a, b is 0.07.

We note again that in constructing the projections of the phase portraits and Poincaré sections for chaotic motion there is the danger of committing the typical error of taking chaotization of a transient process for steady-state chaotic oscillations. Therefore in the discrete values $p_i(\tau)$, $q_i(\tau)$, $\nu(t)$ used to construct the phase portraits and Poincaré sections a large number of values from the initial time of the numerical calculations should be disregarded in order to eliminate distortions in the steady-state phase portraits and sections caused by the trajectories of transient processes.

As the slope angle N_1 of the characteristic of the electric drive decreases further one observes in the system chaos—chaos structural transformations, i.e., a chaotic attractor of one type changes into a chaotic attractor of a different type because of internal bifurcation phenomena.

We consider the types of chaotic attractors existing in the system. For $N_1 = 1.16$ there is a strong transition from the chaotic attrctor shown in Fig. 2a, b to a chaotic attractor of a different type. Projections of the phase portrait and Poincairé section (by the plane $\nu = -11$) of this latter chaotic attractor are shown in Fig. 2d-f for $N_1 = 1.05$. This attractor differs from the preceding one by an increase in the amplitudes of the particularly significant oscillations for ν. The phase trajectories more densely cover the phase volume. The leading Lyapunov exponent of this attractor is 0.22. At $N_1 = 0.99$ there is again a strong chaos—chaos type transition in the system. Figure 3a-c show projections of the phase trajectories and Poincaré section (by the plane $\nu = -11$) of an attractor of this kind for $N_1 = 0.85$. In this type of chaotic motion the Poincaré section loses its band structure and becomes spread out. The form of the projection of the phase portrait onto the (p_2, ν) plane

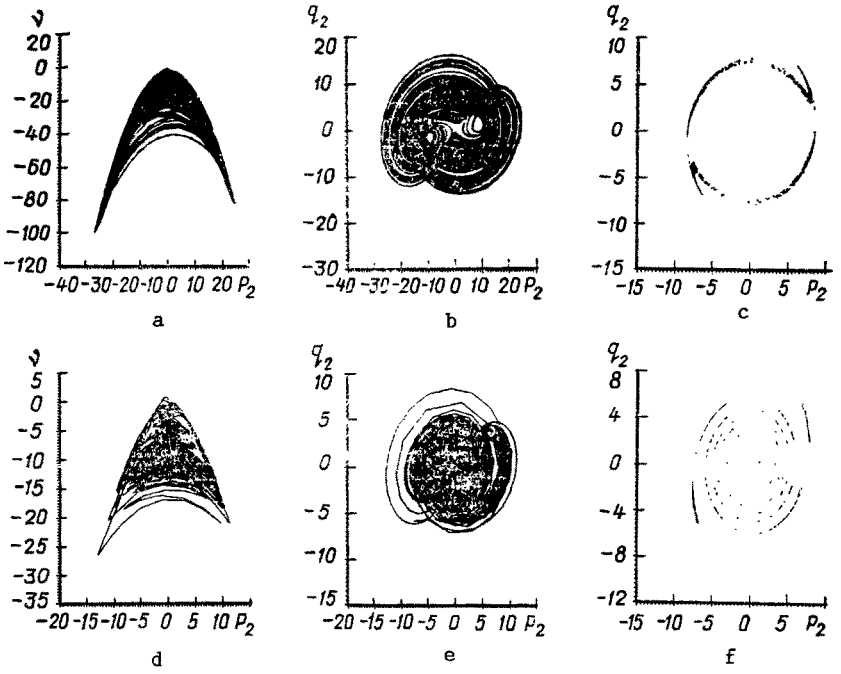

Fig. 3

is quite different. The leading Laypunov exponent of the chaotic attractor shown in Fig. 3a-c is 0.42, which shows the increase in the rate of acceleration of close phase trajectories of this chaotic attractor.

For further decrease in N_1 the projections of the strange attractor begin to be compressed and take the form shown in Fig. 3d-f (for $N_1 = 0.1$). The chaos acquires a structure typical for alternations, i.e., the phase trajectories of the system tend to be attracted to the zero equilibrium state and hence for a long time they wander inside an extremely small neighborhood of this position. Then at an unpredictable time there is a "turbulent explosion" accompanied by nonperiodic motion back along the turns of the spiral of the attractor. The leading Lyapunov exponent of this attractor is 0.20. At $N_1 = 0.08$ the bifurcation process terminates in the equilibrium position $p_1 = q_1 = p_2 = q_2 = 0$; $\nu = 6.25$.

It is interesting to compare our results with a system in which the interaction between the driving force and the vibrational loads is not taken into account. In this case the process is described by a system of equations obtained from (8) as follows. The first equation of (8) is dropped and the unknown function ν in the second, third, fourth, and fifth equations is taken as a constant parameter. The numerical solution for this system was constructed for $\delta = 0.5$, the initial values (10), and values of ν between -250 and 30, which are the limits of the oscillation amplitudes in chaotic motion. The quantity ν was varied using a very small step size. In all cases the approach of the system to the stable equilibrium state was observed and for $|\nu| \geq 3$ the equilibrium position in $p_1 = q_1 = p_2 = q_2 = 0$, $\nu = \text{const}$. In this region of the parameter space not only is chaotic motion not observed, but even limit cycles do not occur. This shows that neglect of the interaction between the vibrational loads and the source of the driving force leads to fundamental errors in the description of the steady motion of the system. The assumed superstable simple regular equilibrium states are actually unstable in the sense of Lyapunov, but stable in the sense of Poisson and are the most complicated examples of chaotic motion.

LITERATURE CITED

1. V. O. Kononenko, Vibrational Systems with Finite Excitation [in Russian], Nauka, Moscow (1964).
2. T. S. Krasnopol'skaya and A. Yu. Shvets, "Chaotic interactions in a pendulum–energy-source system," Prikl. Mekh., 26, No. 5, 90-96 (1990).
3. Yu. I. Neimark and P. S. Landa, Stochastic and Chaotic Vibrations [in Russian], Nauka, Moscow (1987).
4. A. K. Bajaj and J. M. Johnson, "Asymptotic techniques and complex dynamics in weakly nonlinear forced mechanical systems," Int. J. Nonlin. Mech., 25, No. 2/3, 211-226 (1990).

5. G. Benettin, L. Galgani, and J. M. Strelcyn, "Kolmogorov entropy and numerical experiments," Phys. Rev. A, 14, No. 6, 2338-2342 (1976).
6. M. Henon, "On the numerical computation of Poincaré maps," Physica, 5, No. 2, 412-414 (1982).
7. J. W. Miles, "Stability of forced oscillations of a spherical pendulum," Quart. J. Appl. Math., 20, No. 1, 21-32 (1962).
8. J. W. Miles, "Resonant motion of a spherical pendulum," Physica, 11, No. 3, 309-323 (1984).
9. J. W. Miles, "Nonlinear Faraday resonance," J. Fluid Mech., 146, No. 2, 285-302 (1984).
10. J. W. Miles, "Parametric excitation of an internally resonant double pendulum," ZAMP, 36, No. 3, 337-345 (1985).

IMPACT-OSCILLATION MOVEMENT OF A RIGID BODY BETWEEN RECTILINEAR STOPS CONVERGING AT AN ANGLE

R. F. Nagaev and A. K. Khodzhaev

UDC 539.3

Because of the need to study the transient modes of operation of certain types of gyroscopic instruments [1], rotors on magnetic or gas bearings [2], and also ball bearings in the presence of gaps, there arises the problem of the impact-oscillatory motion of rigid bodies in a space bounded by two rectilinear rough surfaces converging at a sharp angle. In the present article this problem is examined in its "plane formulation," with the cases of a rigid body with two translational degrees of freedom (of a material point) and a round body possessing an additional rotational mobility being considered separately. It is assumed that in the intervals between collisions with the stops the body moves rectilinearly through inertia. Collision of the body with the stops is described within the framework of stereomechanical impact theory [3, 4].

The necessary and sufficient conditions of realization of quasiplastic collision [4] – an infinite-impact process of finite duration at the end of which the body arrives at the apex of the angle – are determined.

The Case of a Material Point. If a rigid body undergoes translational, uniform, and rectilinear movement in the intervals between collisions, then, without loss of generality, it may be taken to be a material point. We will assume that the stops are identical to one another in their elastic and dissipative properties, such that the impact interaction with them of a material point is characterized by identical values of the velocity restoration coefficient R and the impact friction coefficient f.

Let us assume that an arbitrary collision of the body with a stop has a nonsliding character and that therefore the vector of its restored velocity is perpendicular to the stop. It is clear that the subsequent impact-oscillatory movement of the body will be characterized by continuous withdrawal from the apex of the angle. Consequently, the above-mentioned quasiplastic impact in this case should be characterized by a sequence of damping sliding collisions [4].

Let us enumerate all collisions of a point with the stops from the beginning of the movement. Then an arbitrary K-th sliding impact (K = 0, 1, 2, ...) will be characterized by the relations

$$v_k = RV_k \sin \vartheta_k, \quad u_k = V_k (\cos \vartheta_k - \varkappa \sin \vartheta_k). \tag{1}$$

Here V_k is the modulus of drop velocity; the angle of its incline to the stop ϑ_k for a quasiplastic impact may be considered as within the interval $(0, \pi/2)$, $\varkappa = f(1 + R)$, while

St. Petersburg, Russia. Translated from Prikladnaya Mekhanika, Vol. 28, No. 10, pp. 68-75, October, 1992. Original article submitted June 7, 1991.

 1063-7095/92/2810-0674$12.50